Supplementary Data

Supplementary Figures

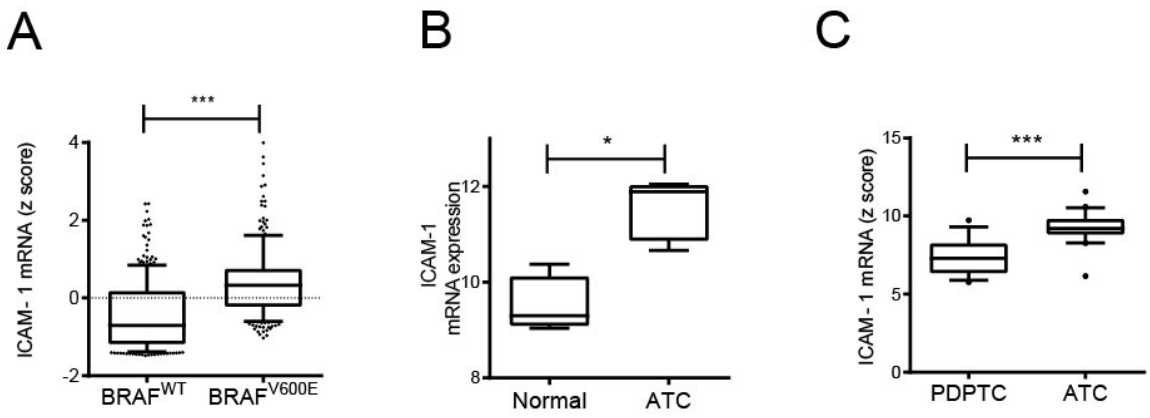

Figure S1. PTCs with BRAF^{V600E} mutations are associated with ICAM-1 overexpression.
(**A**) ICAM-1 mRNA expression levels are compared between PTC patients with the BRAF^{V600E} mutation or BRAF^{WT} using the TCGA database (1). (**B**) ICAM-1 mRNA expression level in patient ATCs is significantly higher than normal thyroid follicles (2). (**C**) Comparison of ICAM-1 mRNA levels between PDPTC and ATC patients (3). Statistical analysis was performed by Mann-Whitney test (***, $p<0.0001$; *, $p<0.05$).

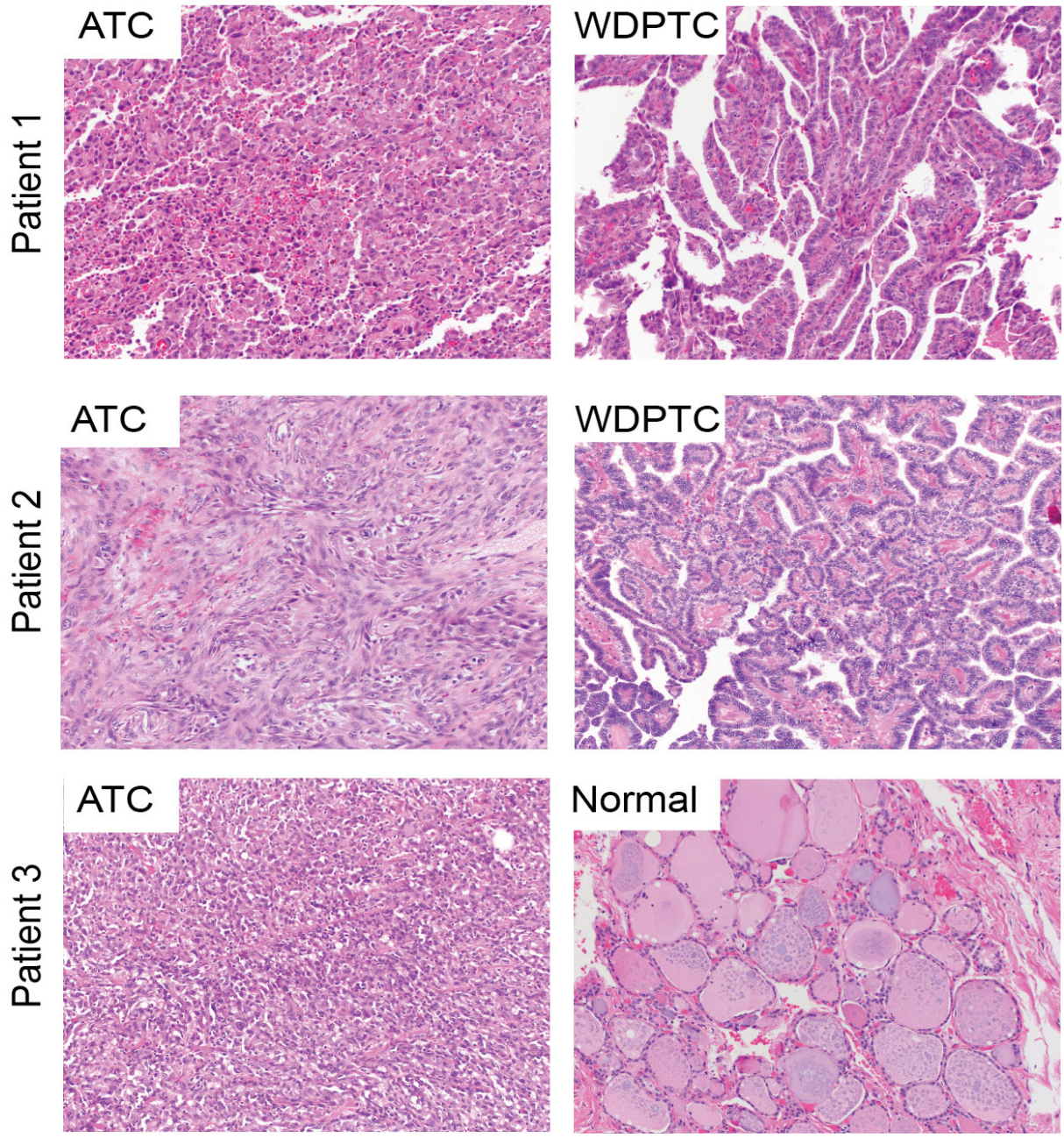

Figure S2. Tumor tissue morphology in ATC patients.
ATC tissue blocks used for ICAM-1 IHC as shown in Fig. 1G were also stained using hematoxylin and eosin. 20X magnification.

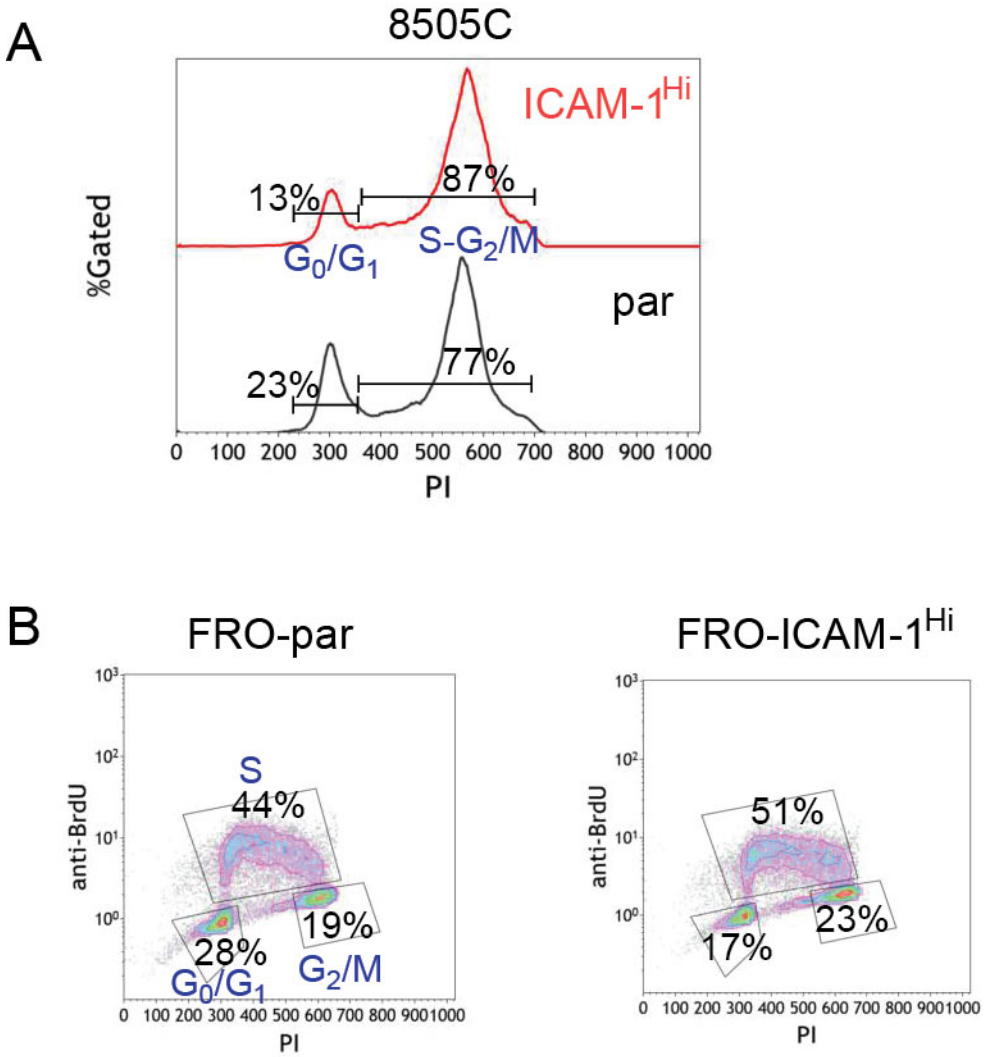

Figure S3. ICAM-1-overexpressing ATC cell lines are more proliferative.
(**A**) Representative flow cytometry histogram plots for cell cycle distribution as measured by propidium iodide (PI) staining of parental (par) 8505C and 8505C cells sorted for ICAM-1 expression (ICAM-1^{Hi}). (**B**) BrdU and PI staining shows an increased fraction of FRO-ICAM-1^{Hi} cells at S and G_2/M phase relative to FRO-par cells.

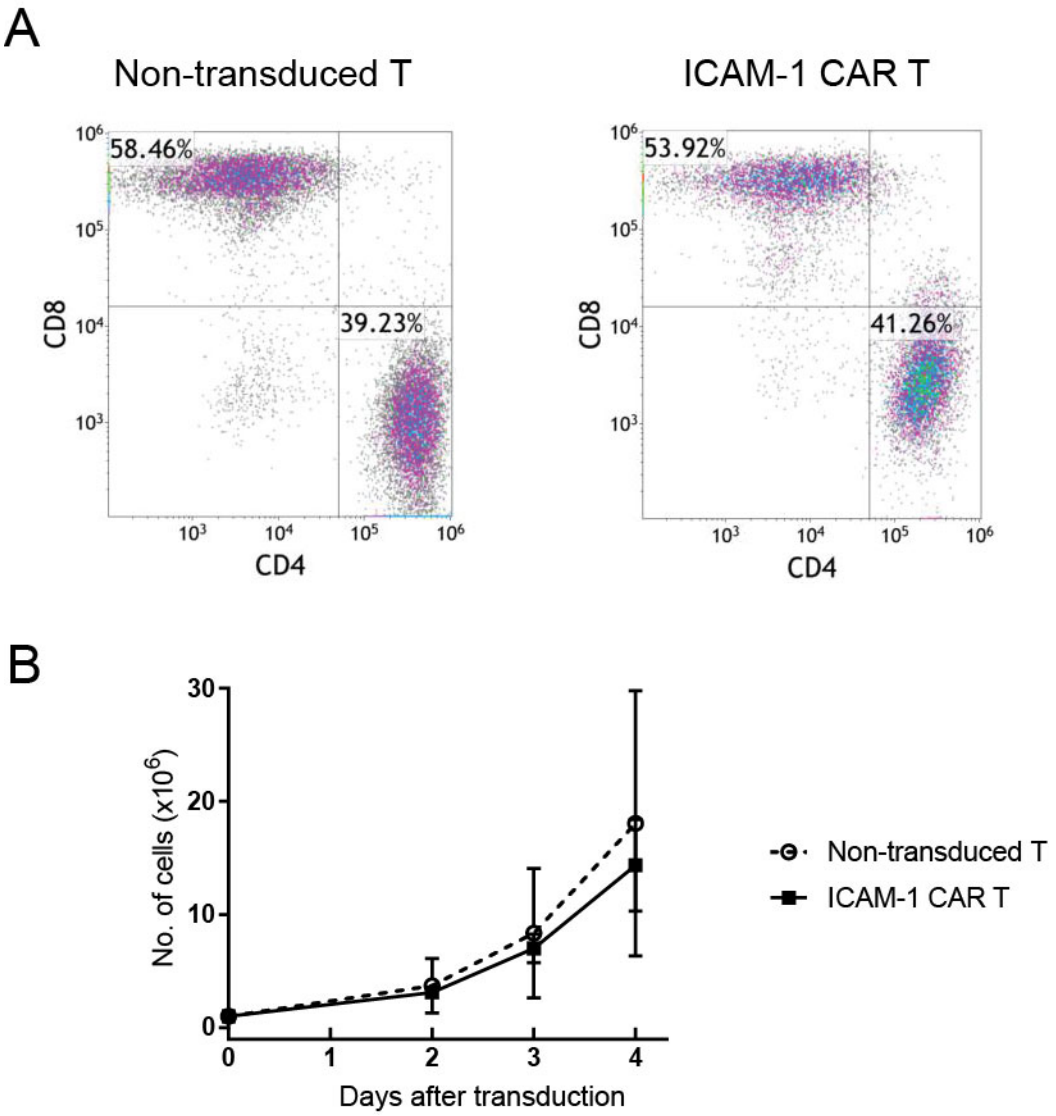

Figure S4. ICAM-1 CAR T cell phenotype characterization.
(**A**) Representative flow cytometry plots showing the composition of $CD4^+$ vs. $CD8^+$ T cells prior to and after ICAM-1 CAR expression in primary T cells. (**B**) The proliferative capacity of T cells after ICAM-1 CAR lentiviral transduction were not statistically different from non-transduced T cells (n=4-5).

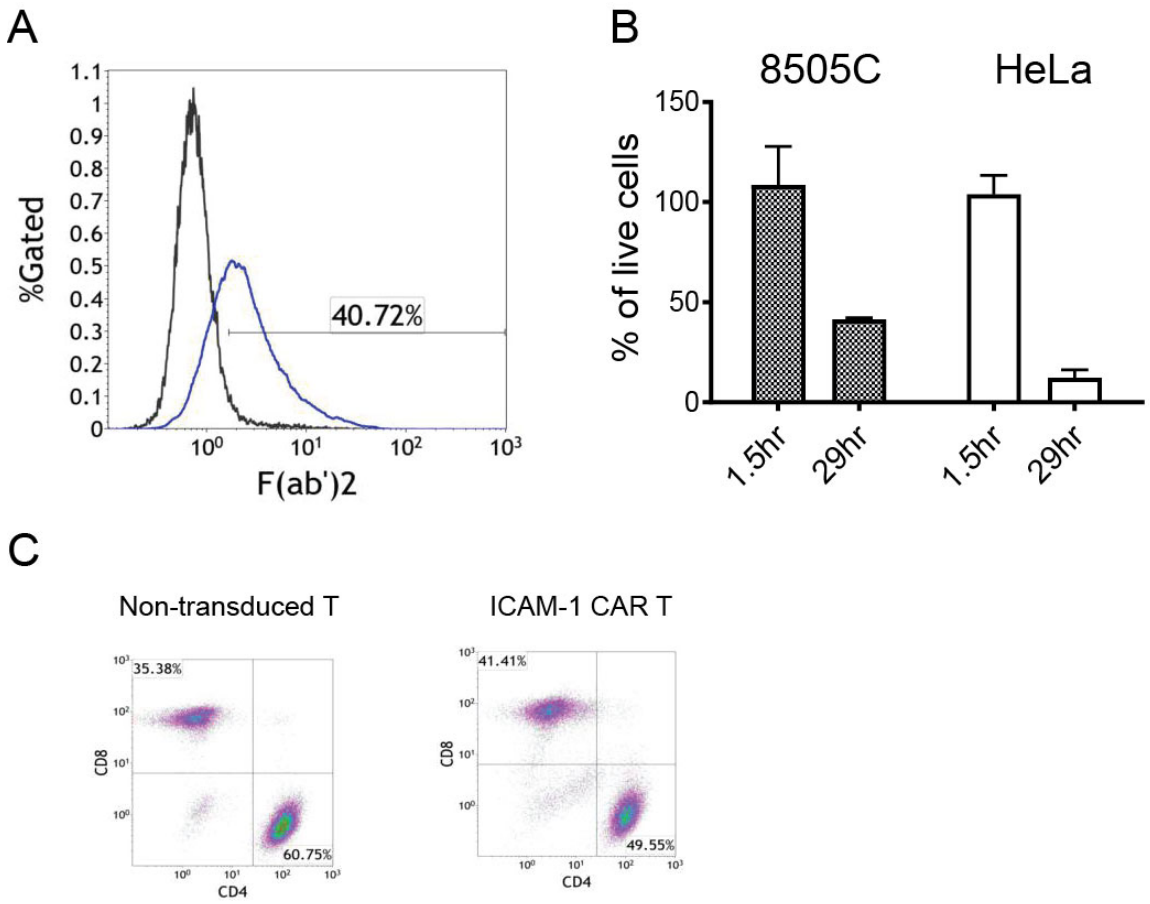

Figure S5. Validation of ICAM-1 CAR T cells used *in vivo* experiments.
(**A**) Transduction rate of ICAM-1 CAR construct in PBMC-derived T cells. (**B**) E:T assay of ICAM-1 CAR T cells against target cells. (**C**) Immunophenotype of non-transduced and ICAM-1 CAR T cells. The ratio of CD4:CD8 T cells were similar prior to and after ICAM-1 CAR expression in primary T cells.

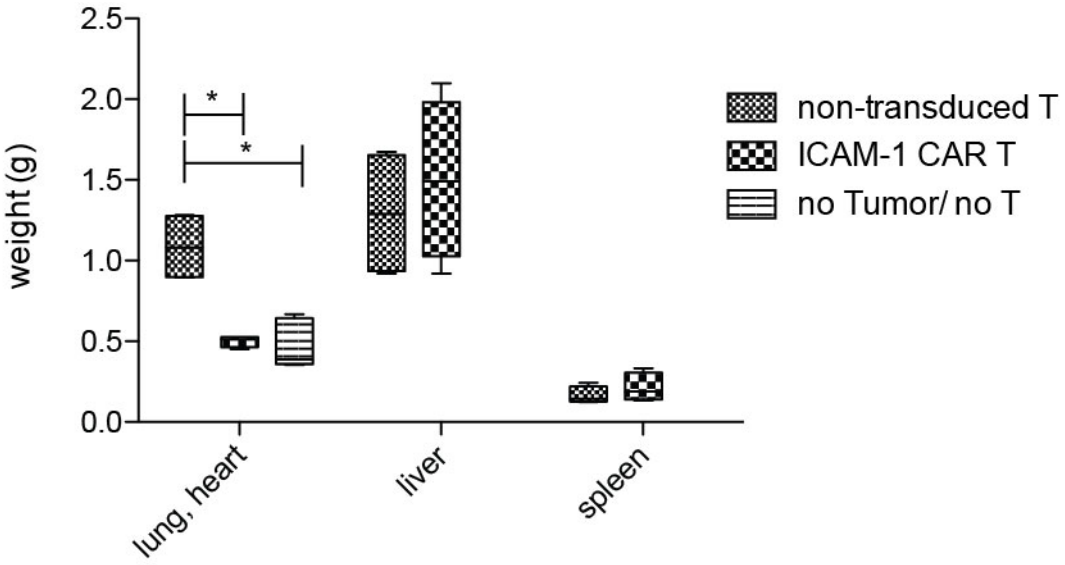

Figure S6. Organ weight changes in ATC xenografted mice after ICAM-1 CAR T treatment.
The weights (g) of lung and heart were significantly reduced in 8505C xenografts treated with ICAM-1 CAR T when compared with non-transduced T cell treatment group and were similar to the weights of healthy organs from NSG mice (no Tumor/No T group) (n=4-6 per group).

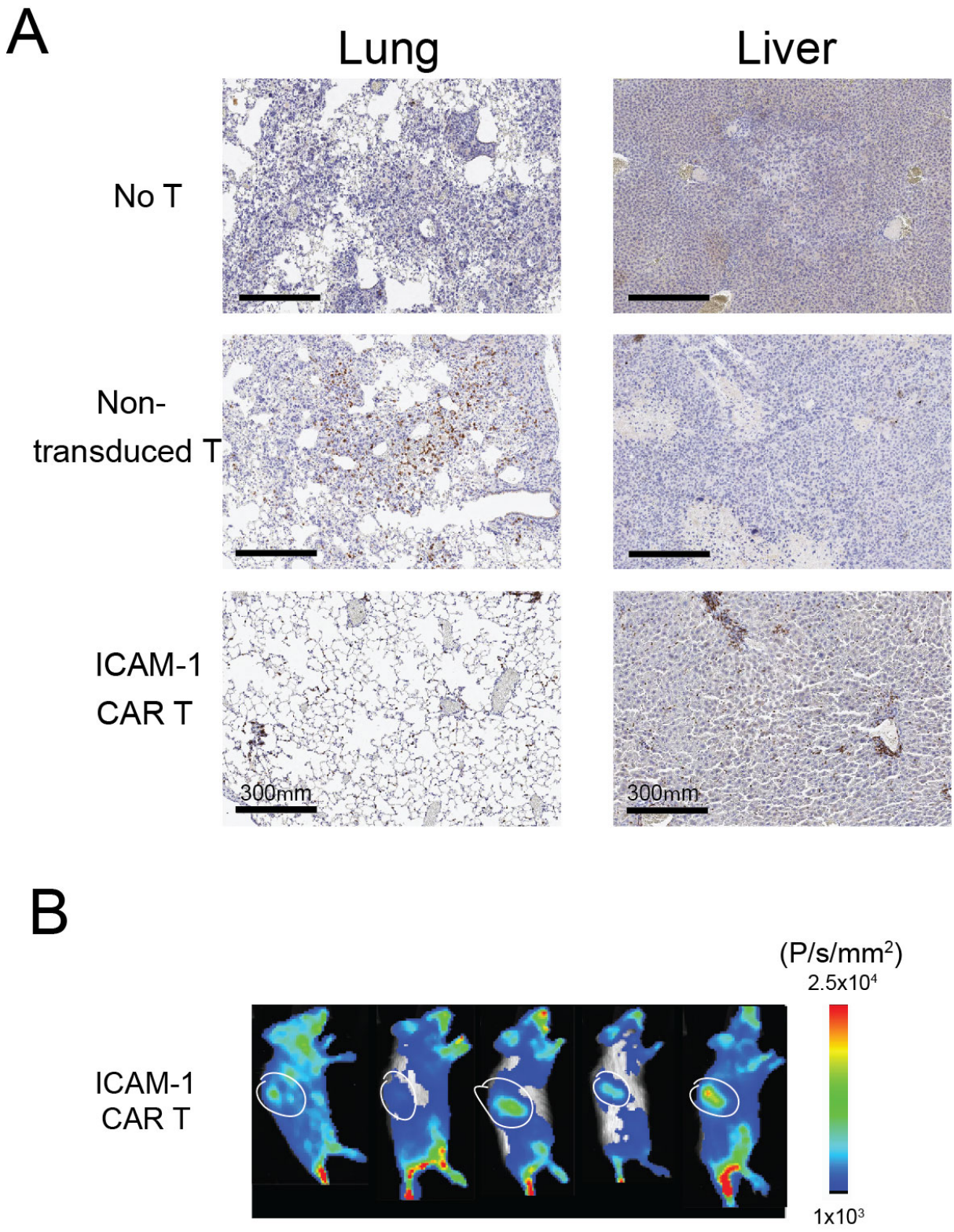

Figure S7. CAR T cells in ICAM-1 CAR T treated and ATC xenografts.
(**A**) Representative CD3 IHC images of T cells in 8505C xenograft tissues treated with ICAM-1 CAR T cells compared to untreated or non-transduced T cell treatment. (**B**) Bioluminescence of rLuc activity is detectable in spleens and other organs of ICAM-1 CAR T-treated mice at X86T72. No detectable rLuc activity is measured in NSG xenografts without treatment or treatment with non-transduced T cells. Spleen is demarcated with a white line.

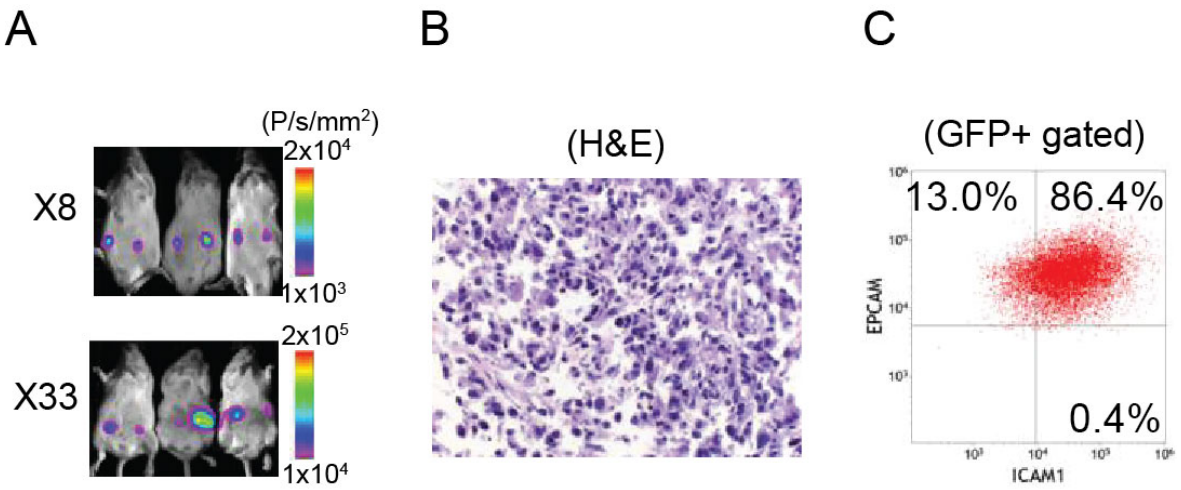

Figure S8. Establishment of ATC patient-derived xenografts.
(**A**) Patient-derived ATC tumors were transduced with GFP and fLuc expressing lentivirus, and subcutaneous bilateral tumor growths in NSG mice were tracked via bioluminescence imaging. (**B**) H & E stained tumor cells with nuclear morphology characteristic of ATC (10X magnification). (**C**) GFP^+ tumor cells from bulk tumor were analyzed for ICAM-1 and EPCAM expression by flow cytometry.

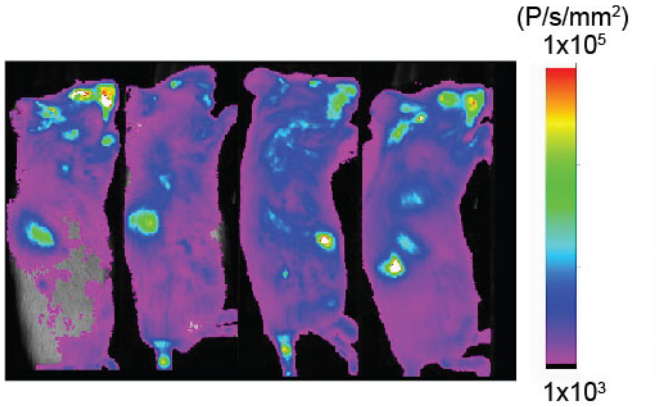

Figure S9. CAR T activity is detectable throughout the body.
Bioluminescence of rLuc activity is detectable in spleens and other organs in ICAM-1 CAR T-treated xenografts at X31T19.

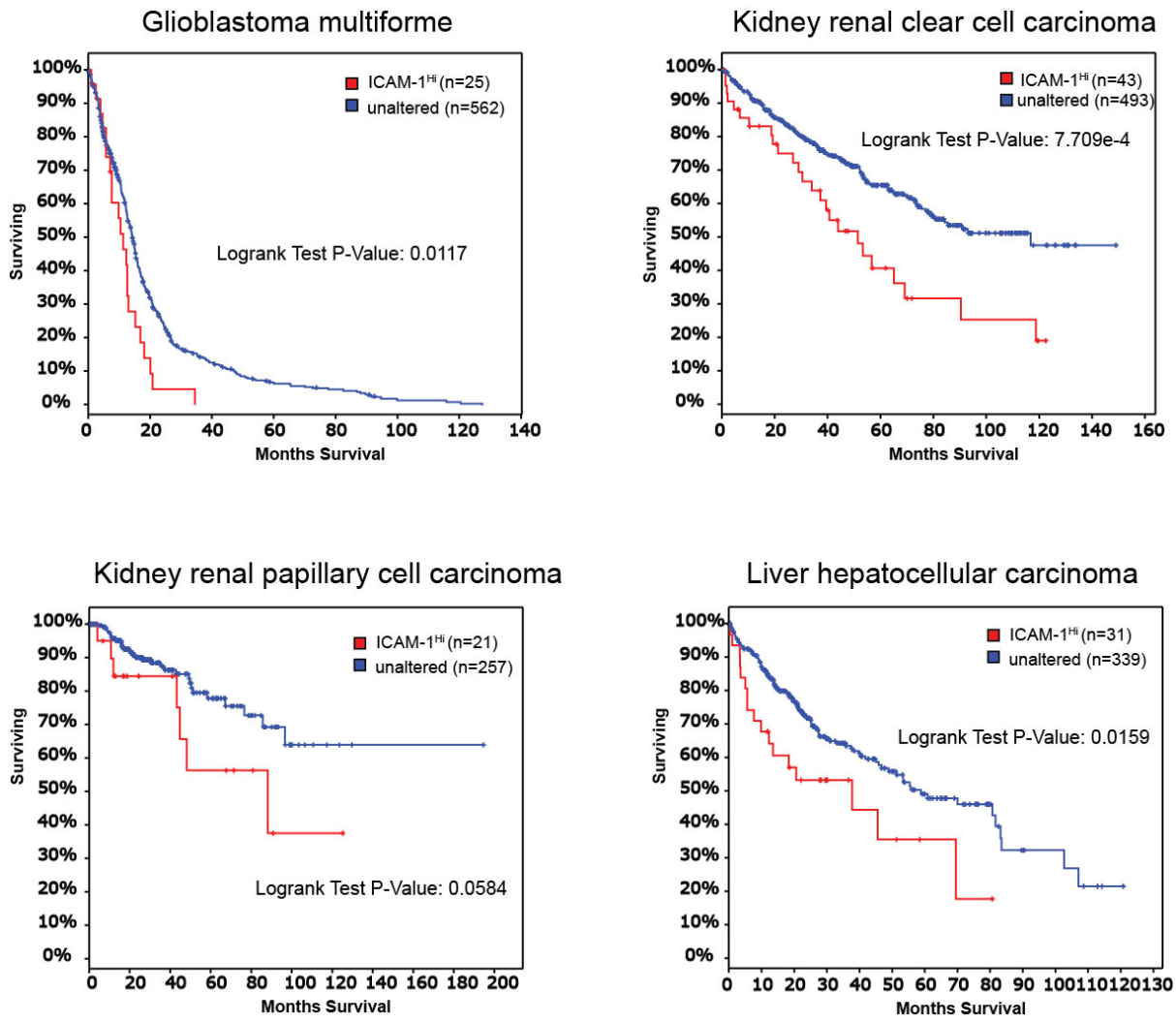

Figure S10. Correlation between ICAM-1 overexpression in TCGA cancer patient tumor tissues and overall survival.
Kaplan-Meier plots demonstrate significant differences between the overall survival rates of patients with glioblastoma multiforme, renal clear cell carcinoma, renal papillary cell carcinoma, and hepatocellular carcinoma with unaltered and ICAM-1-overexpression (Z score>1.5). Clinical information and ICAM-1 expression levels were derived from TCGA datasets (4). Retrospectively, sample size was estimated to be able to detect differences in survival with 80% power using a two-sided, 0.05 alpha level.

Supplementary Methods

Cell lines and Primary cell culture

8505C, BCPAP, FRO, KHM-5M, HEK 293T, and HeLa cells were maintained in RPMI medium supplemented with 10% FBS and 100 U/ml Pen/Strep. HMEC-1 cells were maintained in MCDB131 medium (ThermoFisher) supplemented with 10% FBS, 10 ng/ml Epidermal Growth Factor (ThermoFisher), 1 μg/ml hydrocortisone (Sigma-Aldrich), 10 mM glutamine, and antibiotics. Primary SAEC from healthy donors were cultured in SABM media supplemented with SAGM bullet kit (Lonza). Primary kidney MVEC cells were maintained in CSC complete media, which includes animal derived growth factors (CultureBoost) and 10 % serum (Cell Systems). For certain studies, cell lines were transduced with a fLuc-F2A-GFP lentivirus (Biosettia). Peripheral blood mononuclear cells (PBMCs) were isolated over Ficoll-Paque PLUS (GE Healthcare) and cultured in Optimizer CTS T-cell Expansion SFM (Thermo Fisher) supplemented with 5% human AB serum (Sigma-Aldrich), 2 mM L-alanyl-L-glutamine dipeptide, 100 U/ml Pen/Strep and 30 IU/ml human IL-2 (Cell Sciences). Nonadherent PBMCs were recovered after 24 hours and magnetically enriched for T cells using Dynabeads Human T Expander CD3/CD28 (Thermo Fisher) at a 2:1 bead/T cell ratio. Dynabead-bound T cells were subsequently cultured in IL-2–containing media at a density of 1-2 × 10^6 cells/ml. Surgically resected fresh tumor tissues were finely minced and digested with a mixture of collagenase and hyaluronidase (STEMCELL technologies) at 37°C on a shaker for 1 hour. After gentle washing, tumor tissues were seeded in a 6-well plate in RPMI-1640 media supplemented with 10% FBS and 100 U/ml Pen/Strep.

E:T assay and cytokine analysis

Target cells ($5x10^3$) with fLuc expression were co-cultured with $1.25x10^4$ ICAM-1 CAR-transduced T cells in T cell media containing 150 μg/ml D-luciferin (Gold Biotechnology) with no addition of exogenous cytokines. Luminescence values were measured over time using a TECAN Infinite M1000 PRO plate reader and were normalized to control wells containing tumor and non-transduced parental T cell co-cultures. Supernatants from ICAM-1 CAR T and target cell co-cultures were quantitatively analyzed for the presence of Human IFN-γ and Human Granzyme B using the ELISA MAX™ Deluxe Kit and the LEGEND MAX™ Human Granzyme B ELISA Kit, respectively (both from BioLegend). Supernatant samples were spun for 3 minutes at 300 x *g* to remove debris and stored at -80° C, avoiding freeze/thaw cycles. Exogenous IFN-γ (Peprotech) was added to certain cells for analysis of ICAM-1 induction.

Flow cytometry analysis for protein expression and cell cycle

Staining of cell lines and primary cells was performed on ice for 20 minutes in 1x Hank's buffered saline solution (HBSS) staining solution containing 2% normal goat serum and 0.1% bovine serum albumin. ICAM-1 expression on cell lines and primary tumor cells was determined using a mouse anti-human ICAM-1 R6.5 monoclonal antibody (5μg/ml) that was conjugated in-house to Cy5.5 (Sulfo-Cyanine5.5 NHS ester, Lumiprobe) or with a secondary antibody against FITC-conjugated goat anti-mouse IgG (ThermoFisher) (R6.5 IgG was purified from hybridoma (ATCC))(28). Anti-human CD3-PECy5/CD4-PE/CD8-FITC cocktail, Alexa Fluor 647 anti-human CD3 (HIT3a), PE-conjugated EPCAM, APC-conjugated ICAM-1 (HA58) antibodies were from BioLegend. FITC-conjugated anti-mouse F(ab')2 antibody (ThermoFisher) was used to detect CAR expression in primary T cells. Live cell gating was determined by calcein blue (ThermoFisher) uptake. Organ tissues harvested

from animals were macerated through a 70μm filter and after washing, tissue cell pellets were resuspended in red blood cell lysis buffer (BioLegend) on ice for 20 minutes. Mouse tissue cells were first blocked with mouse IgG (Sigma-Aldrich) at 2 μg/ml for 10 minutes, and then stained with primary antibodies. Dead cells and debris were excluded based on propidium iodide (PI, Sigma-Aldrich) staining at 1μg/ml.

Cell cycle analysis

$5x10^5$ cells were seeded in 6-well plates overnight in RPMI media containing 10% FBS. Media was replaced with 2.5% FBS containing RPMI-1640 media in a subset of wells the following morning, and all cells were harvested and fixed 48 hours later using ice-cold PBS and 70% ice-cold ethanol, sequentially. After fixation at 4°C for 48 hours, cells were washed twice with PBS, treated with 100 ug/mL RNaseA for 30 minutes at 4°C, washed once with PBS, and stained with 50 ug/mL PI. For some experiments, cell cycle was determined by double staining of PI and FITC anti-BrdU antibody (BioLegend) after 30 min of incubation with 1 mM BrdU (Sigma-Aldrich) for 30 minutes. To determine Fas L- or TRAIL-induced cell death, His-tagged recombinant human Fas Ligand (TSFSF6, R&D systems) or TRAIL (TNFSF10, R&D systems) protein was added to the cells in media along with 2 μg/ml of anti-His crosslinking antibody (R&D systems). Flow cytometry data was acquired using a Gallios flow cytometer and was analyzed using Kaluza software (Beckman Coulter).

Cell Proliferation Assay

The Vybrant MTT Cell Proliferation Assay Kit (ThermoFisher) was used to assess cell proliferation. $5x10^3$ viable cells were seeded per well in a 96-well plate in a final volume of

200 µL of RPMI-1640 media supplemented with 10% FBS. After overnight incubation, vemurafenib (Selleck Chemicals) was added to each well at a final concentration of 0.2% in phenol red-free RPMI-1640 media containing 2.5% FBS. After 72 hours, cells were fixed in MTT stock solution, as per manufacturer's instructions. Absorbance was read in an iMARK microplate reader (BioRad) at 490nm. For colony formation assays, $2x10^3$ cells per well were seeded in a 6-well plate. Treatment with vemurafenib was carried out as per the MTT assay. After 72 hours, cells were incubated in regular media for 10 days, followed by methanol fixation and staining with 0.1% crystal violet solution (Sigma-Aldrich).

Immunohistochemistry

Human tumor specimens were collected from patients undergoing surgery at Weill Cornell Medicine/New York Presbyterian Hospital. Formalin-fixed, paraffin-embedded human tissue blocks were cut at 5µm thick intervals and two consecutive slides were stained for ICAM-1 (G-5, Santa Cruz Biotechnology) and hematoxylin and eosin (H&E) at the Translational Research Lab at WCM Pathology and Laboratory Medicine (5). Tumor xenografts were harvested, fixed in 4% paraformaldehyde in PBS, embedded in paraffin, and cut as 5µM sections. For lung tissues, 4% paraformaldehyde solution was perfused into the trachea to preserve the tissue morphology. All five lobes were separated and paraffin fixed. Consecutive slides were stained for H&E, human CD3, and GFP (Histowiz, Brooklyn). An endocrine pathologist (TS) reviewed each case to ensure correct diagnosis and to determine the tumor extent, CD3, GFP, and ICAM-1 staining in patient-derived and cell line xenografted tumor blocks.

TCGA data reanalysis

Clinical parameters, genomics and computational methods are described in detail in (1). The results here are in whole or part based upon data generated by the TCGA Research Network: http://cancergenome.nih.gov/. The level of ICAM-1 RNA expression was given as a Z-score, which is the relative expression of an individual gene within tumor to the gene's expression distribution in a reference population. The ERK activity score is derived from 52 gene-signatures that were responsive to a MEK inhibitor in $BRAF^{V600E}$ melanoma cell lines (6). $BRAF^{V600E}$-RAS score (BRS) determines whether PTC exhibited a transcriptional program that related closer to tumors with $BRAF^{V600E}$ or RAS activating mutations by computing expression of 71 genes (details in (1)). Tumors with negative BRS were defined as $BRAF^{V600E}$-like, while those with a positive BRS were defined as RAS-like. The thyroid differentiation score (TDS) was determined by the relative transcription of 16 different thyroid function genes. Tumors with a positive TDS retain thyroid functions, whereas those with a negative TDS indicates a loss of normal thyroid cell function. Disease-free survival curves and overall survival curves were graphed using the Kaplan-Meier Method and were compared using the log-rank test. We analyzed the 80% power using a two-sided, 0.05 alpha level test to estimate whether the total number of events were sufficient.

Patient-derived ATC xenograft analysis

For tumor burden analysis of patient-derived ATC-xenografts, mice were scanned with a 7T preclinical MRI scanner (Bruker Biospec 70/30 USR). Animals were placed prone headfirst into the system, with a respiratory sensor on their bodies to implement respiratory gating within coil (inner diameter, 3 cm). MR data was acquired with a Rapid Imaging with Relaxation Enhancement (RARE) sequence using the following parameters: echo time =

8.710 milliseconds, repetition time = 1144.512 milliseconds, RARE factor = 2, number of averages = 18, total scan time = 32 minutes, FOV = 30 mm x 30 mm, spatial resolution = 0.117 mm/pixel, matrix size = 256 x 256, slice thickness = 0.5 mm, slices = 48. DICOM files were analyzed using open sourced software ITK-Snap. Tumor burden was calculated as a ratio of volume of tumor over volume of pulmonary cavity excluding heart.

References

1. Cancer Genome Atlas Research N. Integrated genomic characterization of papillary thyroid carcinoma. *Cell.* 2014;159(3):676-90.
2. Pita JM, Figueiredo IF, Moura MM, Leite V, and Cavaco BM. Cell cycle deregulation and TP53 and RAS mutations are major events in poorly differentiated and undifferentiated thyroid carcinomas. *J Clin Endocrinol Metab.* 2014;99(3):E497-507.
3. Landa I, Ibrahimpasic T, Boucai L, Sinha R, Knauf JA, Shah RH, Dogan S, Ricarte-Filho JC, Krishnamoorthy GP, Xu B, et al. Genomic and transcriptomic hallmarks of poorly differentiated and anaplastic thyroid cancers. *J Clin Invest.* 2016;126(3):1052-66.
4. Gao J, Aksoy BA, Dogrusoz U, Dresdner G, Gross B, Sumer SO, Sun Y, Jacobsen A, Sinha R, Larsson E, et al. Integrative analysis of complex cancer genomics and clinical profiles using the cBioPortal. *Sci Signal.* 2013;6(269):pl1.
5. Buitrago D, Keutgen XM, Crowley M, Filicori F, Aldailami H, Hoda R, Liu YF, Hoda RS, Scognamiglio T, Jin M, et al. Intercellular adhesion molecule-1 (ICAM-1) is upregulated in aggressive papillary thyroid carcinoma. *Ann Surg Oncol.* 2012;19(3):973-80.
6. Pratilas CA, Taylor BS, Ye Q, Viale A, Sander C, Solit DB, and Rosen N. (V600E)BRAF is associated with disabled feedback inhibition of RAF-MEK signaling and elevated transcriptional output of the pathway. *Proc Natl Acad Sci U S A.* 2009;106(11):4519-24.